Hindawi Publishing Corporation
EURASIP Journal on Wireless Communications and Networking
Volume 2008, Article ID 317257, 11 pages
doi:10.1155/2008/317257

Research Article

Optimization of Linear Precoded OFDM for High-Data-Rate UWB Systems

Antoine Stephan, Emeric Guéguen, Matthieu Crussière, Jean-Yves Baudais, and Jean-François Hélard

Institute of Electronics and Telecommunications of Rennes (IETR), INSA, 20 Avenue des Buttes de Coesmes, 35043 Rennes, France

Correspondence should be addressed to Antoine Stephan, antoine.stephan@ens.insa-rennes.fr

Received 15 May 2007; Revised 6 September 2007; Accepted 6 November 2007

Recommended by Hikmet Sari

We investigate the use of a linear precoded orthogonal frequency division multiplexing (LP-OFDM) waveform for high-data-rate ultra-wideband (UWB) systems. This waveform applied for the first time to UWB applications is an evolution of the multiband OFDM (MB-OFDM) solution supported by WiMedia-MBOA (MultiBand OFDM Alliance). The aim of this paper is twofold. Firstly, an analytical study of the LP-OFDM waveform allows to find how to efficiently precode an OFDM signal in order to improve the robustness of the system. Secondly, a global system study is led to highlight the benefits of adding a precoding function to an OFDM signal in the UWB context. Different system choices and parameterization strategies are thus proposed. In both analytical and global system studies, the LP component is optimized without channel state information (CSI) at the transmitter side, as in the MBOA solution. To go further, the MBOA constraints are relaxed, and an additional optimization is performed, with a CSI at the transmitter. The analytical and simulation results show that the joint use of linear precoding and OFDM leads to a significant performance increase compared to the MBOA solution. This improvement is due to the precoding scheme that provides better exploitation of the channel diversity.

1. INTRODUCTION

With the release of the ultra-wideband (UWB) spectral mask by the Federal Communications Commission (FCC) in 2002 [1], UWB has attracted considerable interest in the research and standardization communities for wireless communications, due to its ability to provide high-data rate at low cost and relatively low power consumption. However, UWB has to compromise with very stringent regulations since the allocated UWB spectrum from 3.1 to 10.6 GHz overlays other existing spectrum allocations. In order to reduce interference with existing services, the FCC imposed a power spectral density (PSD) limit of −41.3 dBm/MHz.

The IEEE 802.15.3a wireless personal area networks (WPAN) standardization group proposed a very high-data-rate physical layer based on UWB signaling. The main multiple-access techniques considered by the group are a pulse radio transmission using direct-sequence code-division multiple-access (DS-CDMA) [2], and a multiband orthogonal frequency division multiplexing (MB-OFDM). This second solution, which is also known as WiMedia-MBOA (MultiBand OFDM Alliance) [3, 4], will be referred to as MBOA solution in the rest of this paper. The MBOA solution is one of the most promising candidates due to its ability to mitigate interference and to achieve high data rate. Other techniques based on a multicarrier code-division multiple-access (MC-CDMA) scheme have also been proposed in the literature in order to improve the UWB signal robustness against narrowband interference and to reach higher data rate [5].

The purpose of this paper is to propose a new UWB scheme based on the combination of linear precoding (LP) principles with the OFDM waveform of the MBOA solution. The LP process consists in applying precoding matrices or equivalently spreading sequences to various blocks of subcarriers of the multicarrier spectrum [6]. The OFDM parameters of the MBOA solution are maintained in order not to increase the system complexity significantly. The proposed LP-OFDM UWB system is analyzed through two complementary studies: an analytical study and a system study. The analytical study focuses on the optimization of the precoding function. More precisely, the intrinsic characteristics and

capabilities of the precoding function are highlighted and allocation algorithms are developed to improve the system performance. In a second step, we move to a global LP-OFDM system study, taking into account the different functions of the transmission chain, such as the channel coding and interleaving schemes. This system study, complementarily to the analytical one, points out the advantages of appropriately combining the LP component to the MBOA solution. It is hereby expected to obtain better exploitation of the channel diversity yielding system performance improvement.

The rest of the paper is organized as follows. Section 2 briefly introduces the MBOA solution and describes the proposed LP-OFDM system after discussing, from a general point of view, the interests of adding an LP component to the OFDM scheme. Section 3 details the analytical study that finds the optimal configuration of the precoding function in terms of precoding sequence length and number of sequences. This optimization aims at improving the LP-OFDM system robustness. In Section 4, the global system study is presented and different system choices and parameterization strategies are proposed. In particular, the approach followed to handle the precoding component jointly with channel coding is developed and the limitation of the interference generated by the precoding function is studied. Simulation results showing the interest of the proposed LP-OFDM scheme for UWB applications are given and interpreted in Section 5. Finally, Section 6 concludes the paper.

2. SYSTEM DESCRIPTION

2.1. MBOA solution

The MBOA solution divides the UWB spectrum into 14 subbands of 528 MHz each, as illustrated in Figure 1. Initially, most of the studies have been performed on the first three subbands from 3.1 to 4.8 GHz. An OFDM signal can be transmitted on each subband using a 128-point inverse fast Fourier transform (IFFT). Out of the 128 subcarriers used, only 100 are assigned to transmit data. The multiuser access is performed with time-frequency codes (TFC) which provide frequency hopping from a subband to another at the end of each OFDM symbol. Hence, at a given instant, if we consider a 3-user system, each user occupies one of the first three subbands. The TFC allows every user to benefit from frequency diversity over a bandwidth equal to three subbands. Note, however, that when only the first three subbands are considered, conflicts between users appear when a fourth user is added within a piconet, whereas scenarios going up to six simultaneous users have to be considered in practice.

The constellation applied to the different subcarriers is a quadrature phase-shift keying (QPSK). A 64-state convolutional code with a rate varying from 1/3 to 3/4 is used, leading to different data rates from 53.3 to 480 Mbit/s listed in Table 1. For the first two data rate modes, each complex symbol and its conjugate symmetric are transmitted within the same OFDM symbol. Hence, the frequency diversity is exploited within each subband at the cost of a division of the useful transmitted data rate by two. Moreover, a time spreading factor (TSF) of 2 is applied to the modes with data rates between 53.3 and 200 Mbit/s. It consists in transmitting the same information during two consecutive OFDM symbols in order to benefit from better frequency diversity due to the TFC. In addition, to prevent interference between consecutive symbols, a zero padding (ZP) guard interval is inserted instead of the traditional cyclic prefix (CP) used in the classical OFDM systems. The ZP simply consists in trailing zeros.

In brief, the MBOA solution offers potential advantages for high-data-rate UWB applications, such as the signal robustness against channel selectivity and the efficient exploitation of the energy of every signal received within the prefix margin. However, it can be improved by combining precoding schemes with OFDM, as already seen in other contexts, such as cellular [7] and power line communications [8].

2.2. Proposed LP-OFDM system description

In this paper, we propose to add an LP component to the MBOA solution. The resulting LP-OFDM scheme, also known as spread spectrum multicarrier multiple-access (SS-MC-MA) in the wireless context [9], is applied to UWB while respecting the OFDM parameters of the MBOA solution. Hence, the system evolution reduces in practice to the simple addition of a precoding block in the transmission chain, which does not increase the system complexity significantly. In addition, the LP component can be exploited to reduce the peak-to-average power ratio (PAPR) of the OFDM system [10]. Consequently, it is important to note that the radio-frequency front end of the MBOA solution is maintained.

The precoding function can actually be equivalently viewed as a particular spread-spectrum operation and we will often be talking about either precoding or spreading sequences in the sequel. Taking into account the frequency selectivity and the slow-time variations of the UWB channel in an indoor environment, the spreading sequences are applied in the frequency domain. This spreading component improves the signal robustness against frequency selectivity and narrowband interference, since the signal bandwidth could become much larger than the coherence and interference bandwidths. Moreover, it increases the resource allocation flexibility as the spreading code dimension offers an additional degree of freedom [11]. We will assume that orthogonal spreading sequences are used in the proposed system.

The schematic representation of the LP-OFDM signal is depicted in Figure 2. At a given time, K symbols are simultaneously transmitted by the same user on a specific subset of subcarriers and undergo the same distortions, where K is the number of used spreading sequences. It is well known that the spreading operation introduces some interference between the spreading sequences when orthogonality is not maintained. This interference will be herein referred to as self-interference (SI) instead of the classical multiple-access interference (MAI) obtained when the spreading sequences are exploited for multiple user multiplexing (e.g., with MC-CDMA). The SI can actually be easily compensated for by a simple detection with only one complex coefficient per subcarrier.

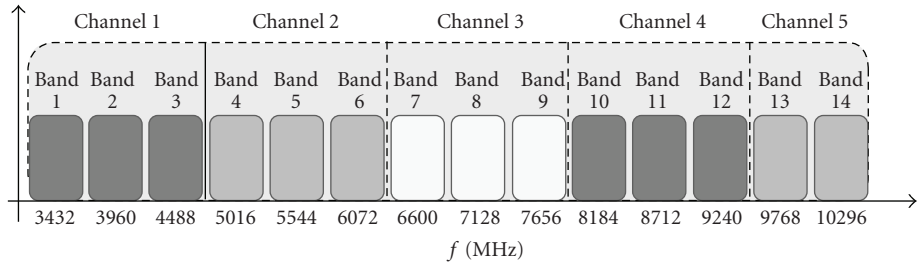

Figure 1: Subbands distribution for MBOA solution.

Table 1: MBOA data rates.

Data rate (Mbit/s)	Modulation	Convolutional coding rate (r)	Conjugate symmetric input to IFFT	Time spreading factor (TSF)	Coded bits per OFDM symbol
53.3	QPSK	1/3	Yes	2	100
80	QPSK	1/2	Yes	2	100
110	QPSK	11/32	No	2	200
160	QPSK	1/2	No	2	200
200	QPSK	5/8	No	2	200
320	QPSK	1/2	No	1	200
400	QPSK	5/8	No	1	200
480	QPSK	3/4	No	1	200

Each user is allocated one of the first three MBOA subbands of 528 MHz bandwidth, in order not to increase the system complexity compared to MBOA. Each subband is then divided into several blocks, each of them including a number of subcarriers equal to the spreading code length L. Note that in Figure 2 the subcarriers linked by the same spreading codes are adjacent to simplify the schematic representation, even if in reality they are not necessarily, as it will be detailed later on.

In addition, when more than three users are considered in the system, the precoding matrix can be exploited to share the same 528 MHz subband between two or even three users. In this case, a generated signal within a given block corresponds to a MC-CDMA signal with a number of two to three users per block, and consequently six to nine users in the system if we consider only the first three MBOA subbands.

In a general approach, the generated symbol vector at the output of the OFDM modulator for an LP-OFDM system can be written as

$$s = F^H M X. \tag{1}$$

Vector s is N-dimensional, with N the number of used subcarriers. $X = [x_1, \ldots, x_K]^T$ is the output of the serial-to-parallel conversion of the K QPSK-mapped symbols to be transmitted. M represents the $N \times K$ precoding matrix applied to X, which precodes K symbols over the N subcarriers. Finally, F^H represents the Hermitian of the $N \times N$ unitary Fourier matrix that realizes the multicarrier modulation. Note that for simplicity reasons, (1) does not involve any guard interval contribution even if a ZP symbol extension is used in practice as in the MBOA solution.

With the proposed LP-OFDM scheme described earlier, the generated symbol vector applied to each subband can be restated as

$$S = F^H D \begin{bmatrix} C_1 & & & \\ & \ddots & 0 & \\ & C_b & & \\ 0 & & \ddots & \\ & & & C_B \end{bmatrix} \begin{bmatrix} X_1 \\ \vdots \\ X_b \\ \vdots \\ X_B \end{bmatrix}, \tag{2}$$

where B is the number of blocks in the subband with $B \times L = N$, C_b the precoding matrix containing the K precoding sequences of block b, and X_b the K-dimensional vector containing the symbols to be transmitted within block b. In addition, a permutation matrix, denoted D, is used to interleave the chips resulting from the precoding process in the frequency domain.

2.3. Channel model

The channel model used is the one adopted by the IEEE 802.15.3a committee for the evaluation of UWB physical layer proposals [12]. This model is a modified version of Saleh-Valenzuela model for indoor channels [13], fitting the properties of measured UWB channels. A log-normal distribution is used for the multipath gain magnitude. In addition, independent fading is assumed for each cluster and each

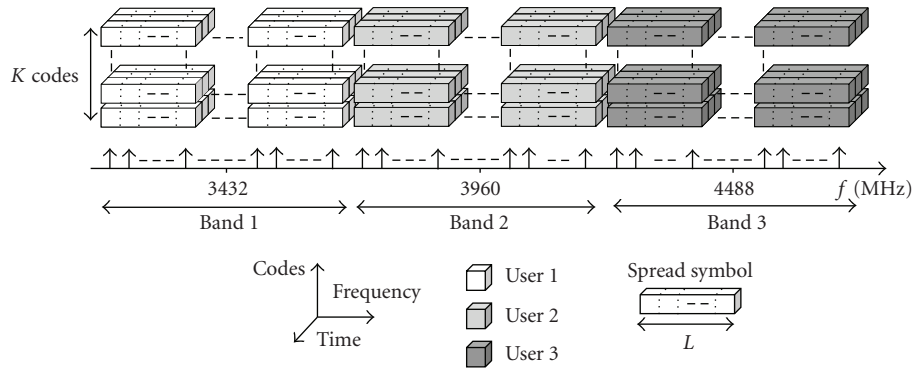

Figure 2: LP-OFDM schematic representation for three users occupying the first three subbands of the MBOA solution.

Table 2: Characteristics of UWB channels.

	CM1	CM2	CM3	CM4
Mean excess delay (ns)	5.05	10.38	14.18	—
RMS delay spread (ns)	5.28	8.03	14.28	25
Distance (m)	< 4	< 4	4–10	10
LOS/NLOS	LOS	NLOS	NLOS	NLOS

ray within the cluster. The impulse response of the multipath model is given by

$$h_i(t) = G_i \sum_{z=0}^{Z_i} \sum_{p=0}^{P_i} \alpha_i(z,p)\,\delta\big(t - T_i(z) - \tau_i(z,p)\big), \quad (3)$$

where G_i is the log-normal shadowing of the ith channel realization, $T_i(z)$ the delay of cluster z, and $\alpha_i(z,p)$ and $\tau_i(z,p)$ represent the gain and the delay of multipath p within cluster z, respectively.

Four different channel models (CM1 to CM4) are defined for the UWB system modeling, each with arrival rates and decay factors chosen to match different usage scenarios and to fit line-of-sight (LOS) and non-line-of-sight (NLOS) cases. The channel models characteristics are presented in Table 2.

3. ANALYTICAL STUDY OF LP-OFDM

As mentioned in the introductive part, this section is dedicated to an analytical study around the LP-OFDM waveform. The objective is to properly handle the linear precoding process so that the system performance is improved. Since we work at target transmission rates in the UWB context, improving the system performance amounts to increasing the system robustness, or equivalently to increasing the system range. As detailed in the previous section, the precoding function can actually be viewed as a particular spread spectrum operation and brings some additional parameters which are the number K of spreading sequences to use, and L their length. These parameters constitute new degrees of freedom in terms of system configuration and can be optimally chosen as proposed in this part. In order to focus on the study of the precoding function, the only LP and OFDM functions are considered here, and other functions of the global transmission chain, as channel coding, for instance, are not taken into account.

3.1. System capacity

Let us first introduce the mathematical expression of the OFDM system capacity. Owing to the orthogonality of the signals, the throughput of an OFDM system in bit per symbol is straightforwardly derived from Shannon Theorem and leads to

$$R_{\text{OFDM}} = \sum_{n\in S} \log_2\left(1 + \frac{1}{\Gamma}\,|h_n|^2 \frac{E_n}{N_0}\right), \quad (4)$$

where S is the group of used subcarriers, Γ the signal-to-noise ratio (SNR) gap of the quadrature amplitude modulation, h_n the frequency-domain response of subcarrier n, E_n the transmitted symbol energy in subcarrier n, and N_0 the noise density.

Whereas a minimum mean square error (MMSE) detector gives better performance, the optimization problem can not be tractable theoretically. Hence, we consider a zero-forcing (ZF) detection in the analytical study. The total throughput in bit per symbol of an LP-OFDM system using ZF detection is given by [14]

$$R_{\text{LP-OFDM}} = \sum_{b=1}^{B} \sum_{k=1}^{K_b} \log_2\left(1 + \frac{1}{\Gamma} \frac{L^2}{\sum_{n=1}^{L} \left(1/|h_{n,b}|^2\right)} \frac{E_{k,b}}{N_0}\right), \quad (5)$$

where B is the number of blocks, K_b the number of codes per block b, L the spreading code length, $h_{n,b}$ the frequency-domain response of subcarrier n in block b, and $E_{k,b}$ the power density of code k within block b. In the UWB case, this power density respects the following condition:

$$\sum_{k=1}^{K_b} E_{k,b} \le E, \quad E_{k,b} \ge 0 \quad \forall b, \quad (6)$$

with E related to the PSD limit defined by the regulation authorities.

The LP-OFDM system optimization is divided into two steps. First, we find the optimal number of blocks that maximizes the system range for a target MBOA throughput. Secondly, we investigate the maximization of the system range

with lower variable throughput, when the previous target throughput is not reachable anymore at high attenuation levels. Note that, a priori, both steps need channel state information (CSI) at the transmitter side, but as we will see later on, only the second step needs CSI at the transmitter.

3.2. Optimization of the number of blocks

We consider N data subcarriers per subband and a fixed QPSK modulation as in the MBOA solution. The objective is to find the optimal number of blocks B, and consequently the optimal spreading code length L, that maximizes the LP-OFDM system range with a fixed target throughput of $2N$ bits per symbol.

By applying Lagrange multipliers to (5) and (6), we find that the optimal solution which maximizes the noninteger system throughput, and consequently the system range, would be to consider

$$E_{k,b} = \frac{E}{K}, \quad K_b = K = L \quad \forall b. \tag{7}$$

Thus, the UWB throughput in bit per symbol becomes

$$R_{\mathrm{UWB}} = 2\sum_{b=1}^{B} L \le \sum_{b=1}^{B} L \log_2\left(1 + \frac{1}{\Gamma}\frac{L}{\sum_{n=1}^{L}\left(1/|h_{n,b}|^2\right)}\frac{E}{N_0}\right). \tag{8}$$

Let γ_b be the noise margin per block b. This margin is an additional SNR gap and can be considered as an amount of extra performance in the presence of unforeseen channel impairments [15]. In our case, it is used to improve the system range.Let

$$|\hat{h}_{n,b}|^2 = |h_{n,b}|^2 \frac{E}{\Gamma N_0}. \tag{9}$$

Hence, using (9) and introducing γ_b in (8), we can write

$$R_{\mathrm{UWB}} = 2N = \sum_{b=1}^{B} L \log_2\left(1 + \frac{1}{\gamma_{\mathrm{b}}}\frac{L}{\sum_{n=1}^{L}\left(1/|\hat{h}_{n,b}|^2\right)}\right),$$
$$\gamma_b = \frac{1}{3}\frac{L}{\sum_{n=1}^{L}\left(1/|\hat{h}_{n,b}|^2\right)} \quad \forall b. \tag{10}$$

Theorem 1. *To maximize the noise margin γ_b of the LP-OFDM system, a code length equal to the total number of useful subcarriers should be used.*

Proof. We want to maximize the minimum value of γ_b. Let α and α_b be such as

$$\gamma_b = \frac{1}{3}\frac{L}{(L/N)\alpha + \alpha_b}, \tag{11}$$

then

$$\sum_{n=1}^{L}\frac{1}{|\hat{h}_{n,b}|^2} = \frac{L}{N}\sum_{b=1}^{B}\sum_{n=1}^{L}\frac{1}{|\hat{h}_{n,b}|^2} + \alpha_b = \frac{L}{N}\alpha + \alpha_b. \tag{12}$$

We have

$$\alpha = \sum_{b=1}^{B}\sum_{n=1}^{L}\frac{1}{|\hat{h}_{n,b}|^2} = \sum_{b=1}^{B}\left(\frac{L}{N}\alpha + \alpha_b\right) = \alpha + \sum_{b=1}^{B}\alpha_b. \tag{13}$$

Thus, we find that

$$\sum_{b=1}^{B}\alpha_b = 0. \tag{14}$$

Let γ be the noise margin of the LP-OFDM system with one block. It can be written as

$$\gamma = \frac{1}{3}\frac{L}{\alpha}. \tag{15}$$

Let b' be such that $\gamma_{b'} > \gamma$, then $\alpha_{b'} < 0$. Hence, $\exists b''$ such that $\alpha_{b''} > 0$, that is, $\gamma_{b''} < \gamma$, and $\min_b \gamma_b < \gamma$. □

Thus, $L = N$ maximizes the noise margin, that is, the optimal solution to maximize the system margin for a given throughput is to use a spreading code length equal to the total number of useful subcarriers.

Consequently, one of the main results of this analytical study is that it is not necessary to know the channel coefficients at the transmitter side to distribute the subcarriers between the blocks, since all these subcarriers are used within the same single block. Furthermore, Theorem 1 shows that the LP-OFDM noise margin can never be lower than the OFDM noise margin. The LP-OFDM system range is therefore larger than the OFDM system range. This result was expected since the LP function provides a better exploitation of the channel diversity.

3.3. Range improvement with variable throughput

Now, we optimize the LP-OFDM system at high attenuation levels when the MBOA target throughput is not reachable. The MBOA constraints are then relaxed and lower throughputs are authorized. We find the optimal configuration of code length L and number K of codes that maximizes the system throughput.

In a general approach with variable throughput, K can be lower than L and Theorem 1 is not applicable anymore. In this case, a multiple blocks configuration has to be considered and each block can exploit its own code length. But finding the optimal block sizes amounts to resolving a complex combinational optimization problem that can not be reduced to an equivalent convex problem. Then, no analytical solution exists and optimal solution can only be obtained following exhaustive search [14]. In order to avoid prohibitive computations, we assume a single block configuration system.

Theorem 2. *Using a fixed QPSK modulation and under a PSD constraint of $\sum_{k=1}^{L} E_k \le E$, the optimal number of codes that maximizes the LP-OFDM margin for a given spreading code length L is equal to $K = \lfloor L(2^{R/L} - 1)/3 \rfloor$, where R is the optimal noninteger single-block throughput given by*

$$R = L \log_2\left(1 + \frac{L}{\sum_{n=1}^{L}\left(1/|\hat{h}_n|^2\right)}\right), \tag{16}$$

where

$$|\hat{h}_n|^2 = |h_n|^2 \frac{E}{\Gamma N_0}. \tag{17}$$

Proof. The LP-OFDM system using the optimal number K of codes should benefit the most from the available energy. Moreover, the system energy can not exceed the PSD limit defined by the regulation authorities and $K \leq L$. Hence, respecting these conditions and using (16) and (5) in the case of a QPSK constellation, K should satisfy the following two equations:

$$\begin{aligned} E - \sum_{k=1}^{K} E_k &= \frac{L}{\alpha}(2^{R/L} - 1) - \frac{K}{\alpha}(2^2 - 1) \geq 0, \\ E - \sum_{k=1}^{K+1} E_k &= \frac{L}{\alpha}(2^{R/L} - 1) - \frac{K+1}{\alpha}(2^2 - 1) < 0, \end{aligned} \tag{18}$$

with

$$\alpha = \frac{L^2}{\sum_{n=1}^{L} (E/|\hat{h}_n|^2)}. \tag{19}$$

Solving (18), we find that the optimal number of codes that maximizes the LP-OFDM range is given by

$$K = \left\lfloor \frac{1}{3} L(2^{R/L} - 1) \right\rfloor. \tag{20}$$

□

The number of codes can never be larger than the spreading code length, and consequently the maximum reachable throughput for a given code length L can be written as

$$\begin{aligned} R(L) &= 2 \times \min\left\{ \left\lfloor \frac{L}{3}(2^{R/L} - 1) \right\rfloor, L \right\} \\ &= 2 \times \min\left\{ \left\lfloor \frac{L^2}{3\sum_{n=1}^{L} (1/|\hat{h}_n|^2)} \right\rfloor, L \right\}. \end{aligned} \tag{21}$$

Finally, the maximum reachable throughput of the LP-OFDM system using the optimal spreading code length and number of codes that maximize the system range becomes

$$R_{\max} = \max_{1 \leq L \leq N} \{R(L)\}. \tag{22}$$

A low-complexity algorithm that derives the optimal number K of codes and the optimal spreading code length is applied to the LP-OFDM system. This algorithm can be advantageously exploited for high-attenuation levels since it increases the system range significantly when the channel response is critical. In addition, these improvements can be obtained without changing the radio-frequency front end of the MBOA solution. This study needs CSI at the transmitter, which is not implemented in the MBOA norm. Consequently, this solution is not considered in the global system study. However, the channel feedback is not difficult to be implemented since the UWB channel response varies slowly in time and can be considered as quasistatic during one frame.

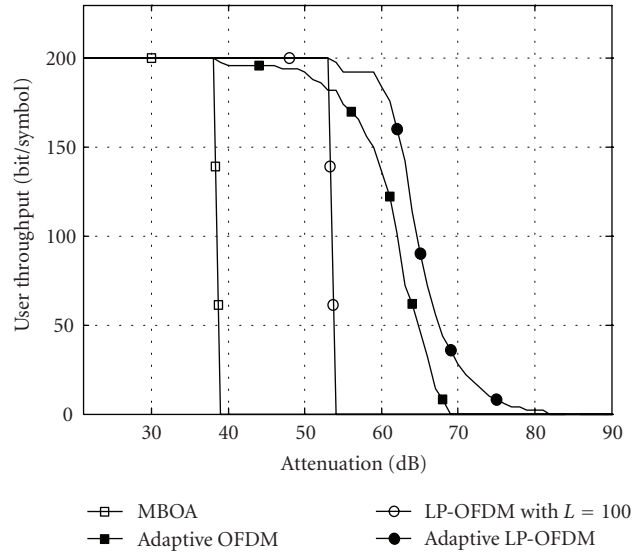

Figure 3: System throughput with the optimal number of codes over channel model CM1.

3.4. Theoretical results

This paragraph presents the results performed on the first three subbands of the MBOA solution, while considering $N = 100$ data subcarriers per subband and a fixed QPSK modulation. The transmitted PSD is $E = -41.3$ dBm/MHz and the noise PSD is $N_0 = -114$ dBm/MHz.

Figure 3 represents the total user throughput per symbol for the different modulation schemes and different attenuation levels, over channel model CM1. The curve "LP-OFDM & $L = 100$" is obtained by applying (8) and Theorem 1, and consequently by using one single block. The curve "adaptive LP-OFDM" is obtained by using (21) and (22) for different attenuation levels. With the OFDM scheme of the MBOA solution, the total throughput of 200 bit/symbol is not reachable at attenuation levels higher than 38 dB, whereas with the proposed LP-OFDM scheme using a single block of length $L = 100$, the user is able to transmit 200 bit/symbol until a 53 dB level (15 dB larger range). Moreover, when we apply the low-complexity algorithm that optimizes the code length and the number of codes for the LP-OFDM system, we are able to transmit data at much higher attenuations (until 81 dB). In addition, the reachable range of this adaptive LP-OFDM scheme is always larger than the range of an adaptive OFDM system. With the called adaptive OFDM scheme, the number of QPSK modulated subcarriers can vary from 100 to 0, whereas with the MBOA solution, the number of active subcarriers is always equal to 100.

Figure 4 gives the optimal values of L and K that maximize the range of the adaptive LP-OFDM system for different attenuation levels, over channel model CM1. The values of K are derived from (20) and the values of L from (21) and (22). We can notice that at high attenuations, the optimal value of K is not necessarily equal to L. Similar results have been obtained with channel models CM2, CM3, and CM4.

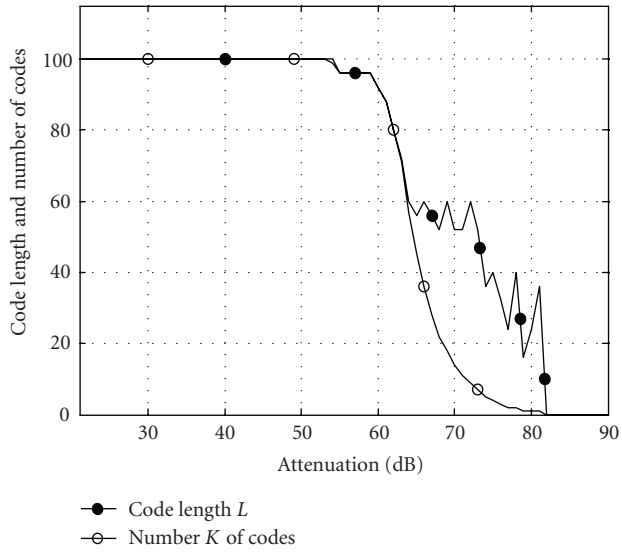

Figure 4: Optimal adaptive LP-OFDM configuration over channel model CM1.

Through this analytical study, we have highlighted the fact that the LP-OFDM waveform has the capability to offer higher robustness, that is, larger noise margins, than the nonprecoded waveform of the MBOA solution. To achieve such improvement, specific algorithms derived in this section have to be applied to get an adequate configuration of the precoding process, namely, in terms of spreading code length and number of codes. The main result to keep in mind for the following is that the optimal solution to maximize the system range for a given throughput is to choose $L = N$. Note that this result strictly holds when no channel coding is used, but it will be very useful to understand and analyze the simulation results obtained in the following section in which the whole transmission system is considered. However, even if a high range gain of about 15 dB has been intrinsically obtained without channel coding by the addition of the LP component, the performance of the two systems will be closer when considering the global chain with channel coding. Finally, the analytical study has been led in the case of ZF detection. We will see later on that the same tendency on the system behavior is obtained in practice with an MMSE detection, especially if the SI experienced within a spreading block has a low variance.

4. GLOBAL LP-OFDM SYSTEM STUDY

4.1. System parameters

After having studied the proposed LP-OFDM scheme through an analytical approach, we move to a global system study taking into account the different functions of the transmission chain, such as the channel coding scheme. The main parameters of the LP-OFDM system are listed in Table 3. Walsh-Hadamard orthogonal spreading codes and MMSE single user detection are applied to limit the SI. Only Sylvester constructions of Hadamard matrices are chosen to simplify the LP-OFDM system. Thus, to compare its performance with different spreading code lengths L, the number of useful subcarriers is reduced from 100 to 96 for each OFDM symbol. Note that the remaining 4 subcarriers could be grouped into an additional block, to use 100 data subcarriers as in the MBOA solution, but this leads to a lower spreading gain.

Table 3: LP-OFDM parameters.

Parameter	Value
IFFT/FFT size	128
Sampling frequency	528 MHz
Transmission bandwidth	490.87 MHz
Number of data subcarriers (N)	96
Number of pilot subcarriers	12
Number of guard subcarriers	10
Total number of used subcarriers	118
Subcarrier frequency spacing	4.125 MHz
IFFT/FFT period	242.4 ns
Zero padding duration	70.08 ns
Symbol interval	312.5 ns
Spreading sequence lengths (L)	1, 4, 8, 16, 32, 64

4.2. Spreading component handling

4.2.1. Spreading block assignment strategy

In LP-OFDM systems, two different frequency assignment approaches can actually be considered to split up the subcarriers into the spreading blocks associated to the precoded symbols.

The first approach is a "standard block interleaving scheme" which consists in interleaving the subcarriers assigned to each spreading block so that the corresponding chips are regularly distributed across the whole bandwidth. Consequently, maximum frequency diversity is made available at the receiver.

The second scheme is called "adjacent subcarrier scheme" as it gathers the chips of one spread symbol from neighboring subcarriers. In contrast to the first scheme, the adjacent subcarrier scheme provides a weaker exploitation of the available frequency diversity. However, the correlation between channel coefficients of adjacent subcarriers is more important, and consequently the channel variance σ_h^2 is smaller. It is proven in [16] that the variance σ_{SI}^2 of the SI is proportional to σ_h^2 over a specific subset of subcarriers, which indicates that using adjacent subcarriers reduces the SI.

Eventually, the "adjacent subcarrier scheme" will be chosen in the sequel in order to limit the SI. In this case, the frequency diversity is jointly exploited by the spreading component and the channel coding combined with bit interleaving.

4.2.2. Spreading code length optimization

The spreading code length L has a direct influence on the LP-OFDM system performance. The longer the spreading codes

are, the more the system takes advantage of the frequency diversity. Moreover, the system flexibility increases with L since the possible number K of spreading codes that can be used also increases, and consequently a larger choice of data rates becomes available. However, the subcarriers of one spreading block undergo a stronger distortion due to the channel selectivity, which induces an increase of the SI. Using shorter spreading code length reduces the SI to the detriment of a weaker channel diversity exploitation by the spreading component. In this case, for low coding rates, the channel decoder is expected to compensate for this lack of diversity exploitation. In other words, the channel coding combined with bit interleaving should allow to fully take benefit of the residual frequency diversity. In opposition, for high coding rates, that is, for coding rates r that tend to 1, the system tends to a noncoded system as the one considered in the analytical study. Consequently, using longer spreading codes may be preferable in order to collect enough diversity, as shown analytically.

4.2.3. Spreading codes selection

In presence of multipath channels, the orthogonality between spreading sequences is destroyed and not completely restored by the MMSE detector. Then, a residual SI term remains. The analytical expression of the SI power associated to a data j in the case of a synchronous LP-OFDM transmission can be expressed as

$$\sigma^2_{\mathrm{SI},j} = \underbrace{(K-1)\,R_j(0)\,L}_{\alpha} + \sum_{\substack{m=1\\ m\neq j}}^{K} \left\{ 2R_j(1) \underbrace{\sum_{n=1}^{L-1} w_n^{(j,m)} w_{n+1}^{(j,m)}}_{\beta_{j,m}} + 2R_j(2) \underbrace{\sum_{n=1}^{L-2} w_n^{(j,m)} w_{n+2}^{(j,m)}}_{\gamma_{j,m}} + \cdots 2R_j(L-1)\, w_1^{(j,m)}\, w_L^{(j,m)} \right\}. \tag{23}$$

R_j is the autocorrelation defined as $R_j(p-q) = E[a_{p,j}\, a_{q,j}]$, where $a_{n,j} = h_{n,j}\, g_{n,j}$ is the coefficient affecting subcarrier n after equalization, with $h_{n,j}$ and $g_{n,j}$ the channel and equalization coefficients, respectively. $w_n^{(j,m)} = c_{n,j}\, c_{n,m}$ represents the product between the chip elements of the spreading sequences used by data j and m on subcarrier n, and $K \leq L$ is the number of active codes.

An optimized spreading code assignment is proposed in [17] to minimize the SI. Judicious subsets of K spreading sequences, whose minimal number of transitions $(+1/-1)$ among each possible product vector $W^{(j,m)} = (w_1^{(j,m)}, w_2^{(j,m)}, \ldots, w_L^{(j,m)})$ is maximum, are selected. In fact, each product vector $W^{(j,m)}$ can have between 0 and $L-1$ transitions. Then, depending on the set of selected spreading sequences, the set of corresponding product vectors has a given minimum which can be different from the minimum of another set. The selected spreading sequences subset is the one whose minimum vectors product is maximal compared to the minimum of the other subsets. In this case, the sum over m of negative terms $\beta_{j,m}$ in (23) decreases, which reduces the SI due to the large positive value α. $W^{(j,m)}$ has to be understood, here, as a measure of the ability to reduce interference between data j and m. With this criterion, the largest degradation among two symbols could be minimized.

5. SYSTEM PERFORMANCE

This section presents the results of the simulations performed on the global LP-OFDM system. The first three subbands of the MBOA solution are being considered. Frames of 150 OFDM symbols are used, and a different channel realization is applied for each frame. The performance is estimated for UWB channel models CM1 and CM2, in the case of perfect channel estimation. Furthermore, the performance of the MBOA solution taking into account the parameters specified in [4] and listed in Table 1 is given as reference.

5.1. Spreading code length effect

The objective is to find the best compromise between the spreading code length L and the coding rate r. We present the system performance obtained versus L: for a given r and a given load K, optimized LP-OFDM systems are simulated for a given E_b/N_0. Three coding rates $r = [1/3\,,\ 1/2\,,\ 3/4]$ and two loads $K = [L/2\,,\ L]$ are considered.

Results are exhibited for channel models CM1 and CM2 in Figure 5. They show that L and r have a strong influence on the LP-OFDM system performance. For low coding rates, the curves tendency shows that it is better to use short code lengths (Figure 5(a)). Reciprocally, the more the coding rate is increased, the longer code the length should be (Figures 5(b) and 5(c)). The use of short spreading code lengths allows to minimize the SI and, combined with a low coding rate, it allows to fully benefit from the channel diversity. At the contrary, when the coding rates increase, the decoder is less able to exploit the channel diversity and longer spreading codes are necessary to compensate for this weakness. Note that for high coding rates, the system tends to a noncoded system. Consequently, the observed behavior is consistent with the conclusions already drawn in the analytical study which shows that the performance of the LP-OFDM system without channel coding are optimal with L set to its maximal value to benefit from the maximum of diversity.

5.2. LP-OFDM system performance with $L = 16$

In Figure 6, $L = 16$ was chosen to assess the performance of the LP-OFDM system since it seems to be a good compromise for the used coding rates, according to the previous results. The joint assignment of the load, that is, the number K of spreading codes, and the coding rate r provide different data rates. Table 4 gives the load/coding rate combinations that lead to LP-OFDM data rate values that are very close to the ones of the MBOA solution. Figure 6 exhibits the results obtained for the data rates of Table 4. In addition, to emphasize on the performance gain at low data rate, Figure 7 exhibits comparative results of the two systems. The plotted curves give for each targeted data rate the E_b/N_0 required to

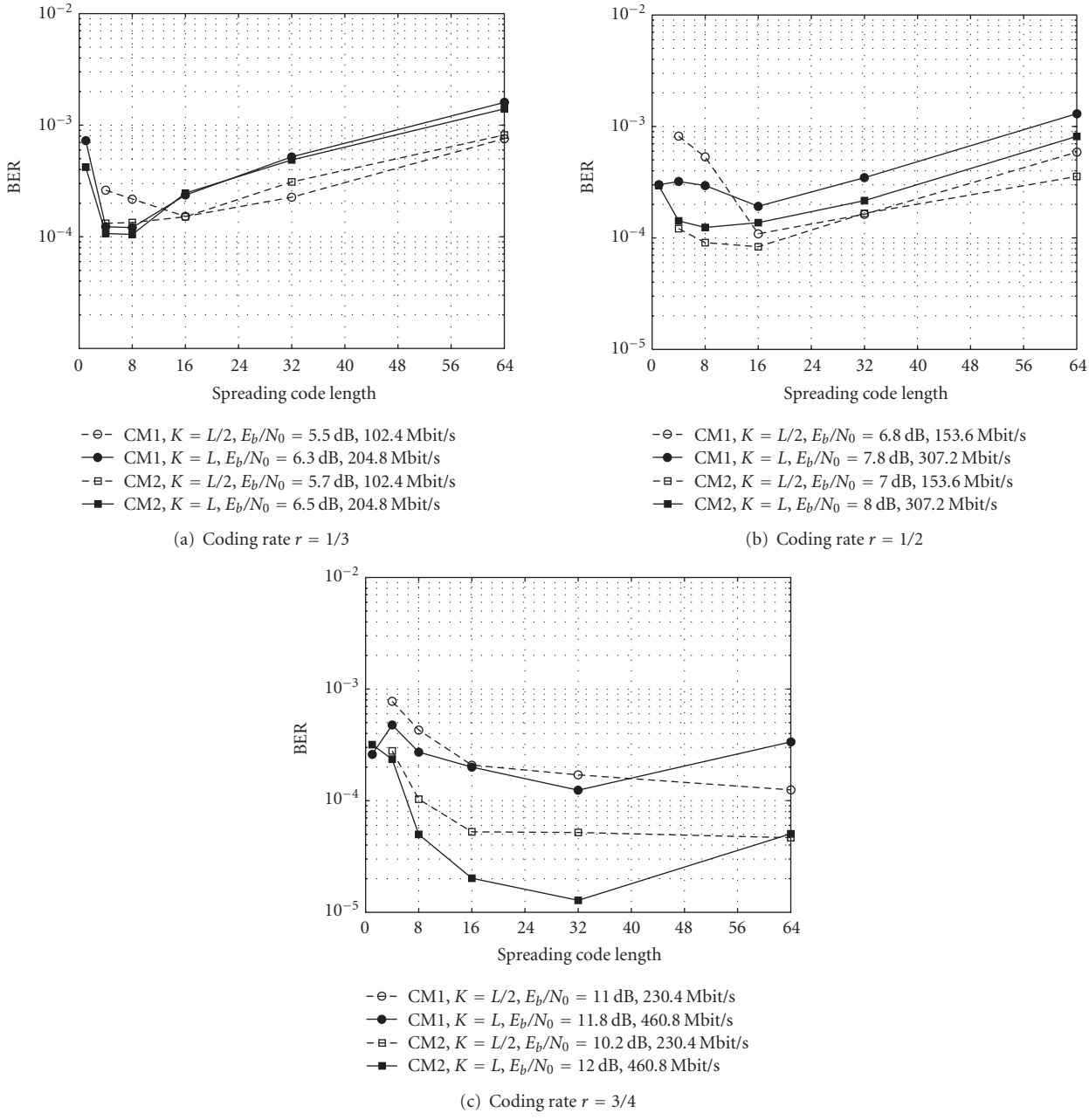

(a) Coding rate $r = 1/3$

(b) Coding rate $r = 1/2$

(c) Coding rate $r = 3/4$

Figure 5: LP-OFDM system performance versus the spreading code length for channel models CM1 and CM2.

obtain a bit error rate (BER) equal to 10^{-4}. Please note that for both systems, the 64-state convolutional code specified in [4] is used to fairly compare the performance. Two coding rates 1/3 and 1/2 are considered with LP-OFDM, and the load K of each considered data rate is mentioned in brackets next to each marker.

Firstly, for LP-OFDM with data rates lower than 200 Mbit/s, a coding rate of $r = 1/3$ should be exploited instead of a coding rate of $r = 1/2$. In fact, an E_b/N_0 gain of more than 1 dB can be obtained with $r = 1/3$, whereas with $r = 1/2$, the MBOA and LP-OFDM systems have very close performances. This global LP-OFDM system gain of around 1 dB is lower than the precoding function gain of the analytical study, since the added coding component squeezes the results considerably. Note that the performance of the MBOA system is better than the LP-OFDM one with $r = 1/2$ for the two data rates 53.3 Mbit/s and 110 Mbit/s. This is due to the lower MBOA coding rates at these two points ($r = 1/3$ and $r = 11/32$, resp.; see Table 1). These results essentially highlight that the MBOA solution based on TSF and conjugate symmetric is not efficient. In addition, for data rates higher than 200 Mbit/s, the LP-OFDM performance with $r = 1/2$ is also better than MBOA. More generally, the proposed system is able to provide a wider range of data rates due to the high flexibility brought by the joint assignment of the number of used codes and coding rates.

Table 4: Possible data rates with LP-OFDM.

Data rate (Mbit/s)	Modulation	Convolutional coding rate (r)	Load (K)	Coded bits per symbol
51.2	QPSK	1/3	4	48
76.7	QPSK	1/3	6	72
115.1	QPSK	1/3	9	108
153.6	QPSK	1/3	12	144
192	QPSK	1/2	10	120
307	QPSK	1/2	16	192
409	QPSK	2/3	16	192
460	QPSK	3/4	16	192

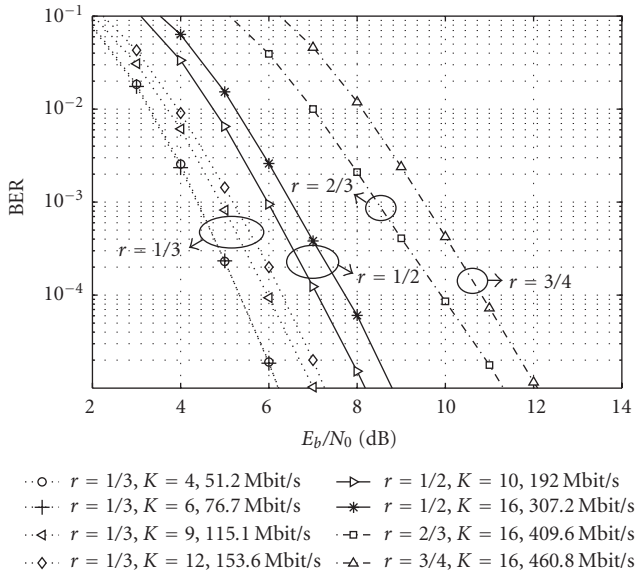

Figure 6: LP-OFDM performance with channel model CM1.

6. CONCLUSION

In this paper, we have proposed a linear precoded multicarrier waveform, called LP-OFDM, for high data rate UWB applications. This scheme applied for the first time to UWB is introduced as an extension of the already established MBOA solution and does not increase the system complexity significantly. The analytical study led on the LP-OFDM waveform has shown that the proposed system is able to outperform the MBOA system in terms of robustness, that is, noise margin. The reason of this improvement is the better exploitation of the channel diversity due to the precoding, or equivalently, the spreading process. The global system study has brought comparable results, showing the advantage of adding a precoding component to the MBOA solution, in terms of performance and flexibility. Merging the conclusions of the analytical and system studies, we showed that the benefits of the spreading and channel coding functions on the channel diversity exploitation are complementary and depend on each other. More precisely, the general tendency is to increase the length of the spreading codes as long as higher coding rates are considered. Consequently, the proposed LP-OFDM system can be advantageously exploited for UWB applications, without implying a substantial increase in complexity.

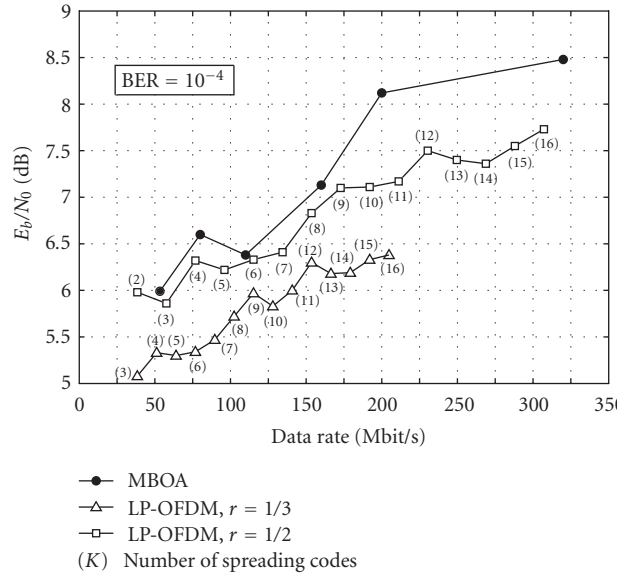

Figure 7: Required E_b/N_0 for a BER = 10^{-4} with channel model CM1.

ACKNOWLEDGMENT

The authors would like to thank France Télécom R&D/RESA/BWA which supports this study within the Contract 46136582.

REFERENCES

[1] "First report and order, revision of part 15 of the commission's rules regarding ultra-wideband transmission systems," ET Docket 98-153, February, 2002.

[2] Q. Li and L. A. Rusch, "Multiuser detection for DS-CDMA UWB in the home environment," *IEEE Journal on Selected Areas in Communications*, vol. 20, no. 9, pp. 1701–1711, 2002.

[3] IEEE P802.15 Working Group for Wireless Personal Area Networks (WPANs), "Multi-band OFDM physical layer proposal for IEEE 802.15 task group 3a," September 2004.

[4] A. Batra, et al., "Multi-Band OFDM physical layer proposal for IEEE 802.15 task group 3a," IEEE document P802.15-04/0493r1, Texas Instruments et al., September 2004.

[5] M. Schmidt and F. Jondral, "Ultra Wideband Transmission based on MC-CDMA," in *IEEE Global Telecommunications Conference (GLOBECOM '03)*, vol. 2, pp. 749–753, San Francisco, Calif, USA, December 2003.

[6] Z. Wang and G. B. Giannakis, "Linearly precoded or coded OFDM against wireless channel fades?" in *IEEE 3rd Workshop on Signal Processing Advances in Wireless Communications (SPAWC '01)*, pp. 267–270, Taiwan, China, March 2001.

[7] S. Kaiser, "OFDM code-division multiplexing in fading channels," *IEEE Transactions on Communications*, vol. 50, no. 8, pp. 1266–1273, 2002.

[8] J.-Y. Baudais and M. Crussière, "Resource allocation with adaptive spread spectrum OFDM using 2D spreading for power line communications," *EURASIP Journal on Advances in*

Signal Processing, vol. 2007, Article ID 20542, 13 pages, 2007.

[9] S. Kaiser and K. Fazel, "Flexible spread-spectrum multi-carrier multiple-access system for multi-media applications," in *Proceedings of the IEEE International Symposium on Personal, Indoor and Mobile Radio Communications (PIMRC '97)*, vol. 1, pp. 100–104, Helsinki, Finland, September 1997.

[10] S. Nobilet, J.-F. Hélard, and D. Mottier, "Spreading sequences for uplink and downlink MC-CDMA systems: PAPR and MAI minimization," *European Transactions on Telecommunications*, vol. 13, no. 5, pp. 465–474, 2002.

[11] A. Stephan, J.-Y. Baudais, and J.-F. Hélard, "Adaptive spread spectrum multicarrier multiple-access for UWB systems," in *proceedings of the 65th IEEE Vehicular Technology Conference (VTC '07)*, pp. 2926–2930, Dublin, Ireland, April 2007.

[12] J. Foerster, et al., "Channel modeling sub-committee report final," IEEE802.15-02/490, November 2003.

[13] Q. H. Spencer and A. L. Swindlehurst, "Some results on channel capacity when using multiple antennas," in *Proceedings of the 52nd IEEE Vehicular Technology Conference (VTC '00)*, vol. 2, pp. 681–688, Boston, Mass, USA, September 2000.

[14] M. Crussière, J.-Y. Baudais, and J.-F. Hélard, "GEN01-5: adaptive linear precoded DMT as an efficient resource allocation scheme for power-line communications," in *IEEE Global Telecommunications Conference (GLOBECOM '07)*, pp. 1–5, San Francisco, Calif, USA, November 2006.

[15] J. M. Cioffi, "A multicarrier primer," ANSI T1E1.4/91–157, Committee contribution, November 1991.

[16] L. Cariou and J.-F. Helard, "A simple and efficient channel estimation for MIMO OFDM code division multiplexing uplink systems," in *IEEE 6th Workshop on Signal Processing Advances in Wireless Communications (SPAWC '05)*, pp. 176–180, York, NY, USA, June 2005.

[17] D. Mottier and D. Castelain, "Spreading sequence allocation procedure for MC-CDMA transmission systems," in *Proceedings of the 52nd Vehicular Technology Conference (VTC '00)*, vol. 3, pp. 1270–1275, Boston, Mass, USA, September 2000.